# The Origin of Saturn's Rings Revisited

Luís Teodoro[1]*, Jacob Kegerreis[2], Paul Estrada[3], Jeff Cuzzi[4], Vincent Eke[2], Richard Massey[2], Matija Ćuk[4], [1]BAERI/NASA Ames Research Center, Moffett Field, CA, USA; [2]Institute for Computational Cosmology, Durham University, Durham, DH1 3LE, UK; [3]SETI Institute, Mountain View, CA 94043; [4]NASA Ames Research Center, Moffett Field, CA, USA. *luis.f.teodoro@nasa.gov

**Introduction:** The apparent geological youth of Saturn's rings is an open question since the days of Voyager [1, 2]. Two models have been suggested: *i)* these rings are primordial and their masses are comparable to the mass of Mimas [1]; and *ii)* the Saturnian rings are young. In the former, it is rather difficult to account for the low observed level of non-icy "pollution" and the substantial observed color variations within the rings given the deposition of meteoroid mass and ballistic transport mixing of micrometeoroid impact ejecta over these long time scales [3, 4]. While the observations gathered during Cassini's final orbits will be needed to remove remaining uncertainties, all recent studies continue to support a ring age on the order of $\sim 10^8$ years [3, 5, 6], far less than what current "primordial" origin scenarios for the rings predict [7].

In the latter case where the rings are young, then either the tidal disruption or collisional destruction of an icy moon must be responsible for their creation. The current flux of heliocentric objects is low [8, 9, 10, 7]. making it much more likely that the ring material originated in the Saturn system. At the moment, this hypothesis of a recent origin of the mid-sized satellites and rings of Saturn is under close scrutiny. Central to this discussion are the collisions between mid-sized objects ($M \sim 10^{19}$–$10^{21}$ kg) resulting from the destabilization of a previous mid-sized moon system that could potentially provide a pathway to the formation of rings and re-accreted moons $\sim$100 Myr ago [11].

**Methods:** To explore the colliding moons scenario, [12] used smoothed particle hydrodynamics (SPH) simulations to investigate the outcome of collisions between two proto-Rhea-sized bodies ($M_{\rm Rhea} \sim 10^{21}$ kg) at an impact velocity of 3 km s$^{-1}$ over several impact angles, but used only $2 \times 10^5$ SPH particles, and only modeled the initial impact. Here we present results from a new suite of high resolution SPH simulations modeling impacts between Saturn's icy mid-sized moons.

This new suite of simulations utilizes the next-generation hydrodynamics and gravity code SWIFT (SPH With Inter-dependent Fine-grained Tasking; swift.dur.ac.uk) [13] with the relevant Tillotson equations of state (EoS) for granite and water ice [14] to track the dynamical evolution of $10^5$–$10^7$ SPH particles within the simulation volume. Briefly, SWIFT uses a fast multipole method (FMM) to calculate gravitational forces between nearby particles. These forces are then combined with a long-range counterpart provided by a mesh to account for more distant particles. Several hydrodynamics schemes are implemented in SWIFT, including the simplest energy-conserving SPH scheme [15] that is employed in this abstract.

In the rest frame of the target, the impactor's initial speed is set to 3 km s$^{-1}$. Both impactor and target are differentiated bodies with a silicate core and water-ice mantle.

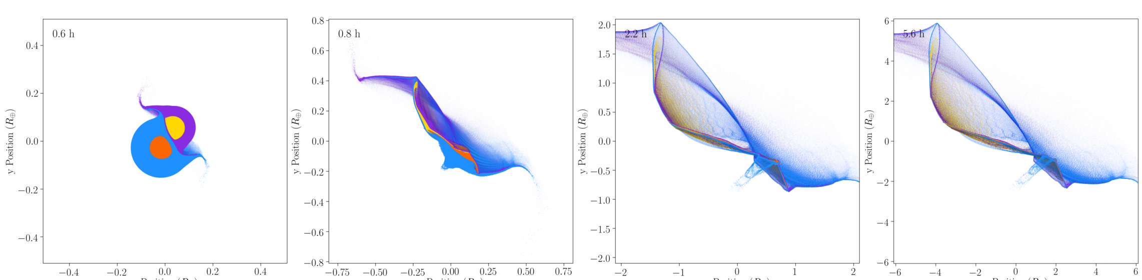


Figure 1: Snapshots [0.6, 0.8, 2.2 and 5.6 h from the beginning of the simulation] showing the provenance of an impact between a Rhea- and Dione-like object. Time increases from the left to the right. The particles are colored by their material: blue and orange represent the rocky core and icy mantle of the Rhea-like body and yellow and purple show the same for the Dione-like object. The number of particles within the simulation box is $N \sim 1.5 \times 10^7$. Each panel has a different length scale, see the axis labels.

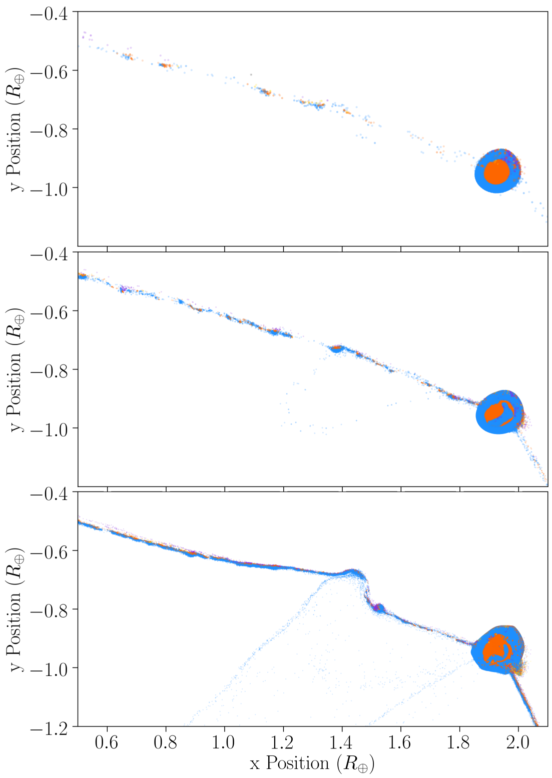


Figure 2: The same three 5.6 h snapshots shown in Figure 1, zoomed-in around the largest moon fragment, to highlight the new details that can be resolved with the higher resolution simulations. The color scheme is the same as in Figure 1.

We sample the parameter space spanned by the impact angle and the ratio between the mass of the impactor to the mass of the target. In our suite of simulations this ratio spans from 0.005 to 1.0, which encompasses Enceladus-Rhea to Rhea-Rhea impacts. Figure 1 shows a snapshot of an impact between a Rhea- and Enceladus-like object. From these higher resolution simulations we can not only determine the number of bound objects and their post-collision trajectories, but also their internal states. This enables continued modeling both of the dynamical evolution of the system and of any impact-driven differentiation from internal thermodynamic evolution, especially for grazing, hit-and-run-type collisions.

To identify objects within the simulation volume we applied a friends-of-friends (FoF) method [16]. This algorithm effectively groups particles bounded by an isodensity surface.

**Initial Results and Discussion:** Amongst our initial results obtained from the higher resolution simulations analysis we have found that there is a myriad of distinct objects. This is in contrast with the lower resolution [12] study. As shown in Figure 2, which zooms in to the region around the largest fragment of the target, high resolution simulations with $10^7$ SPH particles reveal a great amount of structure aside from the largest core fragments. However, simulations with only $\sim 10^5$ particles fail to resolve these details.

We have assessed the range of collisional outcomes while self-consistently modeling satellite dynamical and internal evolution, exploring the degree to which collisional heating and tidal dissipation can soften their interiors, or even lead to some level of differentiation. We are now studying the production rate, composition, and radial distribution of rubble disks in the Saturn system.

## References


[1] L. W. Esposito. *Icarus*, 67:345–357, September 1986.
[2] J. E. Colwell. *Planet. Space Sci.*, 42:1139–1149, December 1994.
[3] P. R. Estrada, et al. *Icarus*, 252:415–439, May 2015.
[4] P. R. Estrada, et al. *Astrophys. J.*, 818:200, February 2016.
[5] Z. Zhang, et al. *Icarus*, 294:14–42, September 2017.
[6] Z. Zhang, et al. *Icarus*, 281:297–321, January 2017.
[7] S. Charnoz, et al. page 537. 2009.
[8] W.-H. Ip. *Astron. Astrophys.*, 199:340–342, June 1988.
[9] J. J. Lissauer, et al. *J. Geophys. Res.*, 93:13776–13804, 1988.
[10] L. Dones. *Icarus*, 92:194–203, August 1991.
[11] M. Ćuk, et al. *Astrophys. J.*, 820:97, April 2016.
[12] R. Hyodo and S. Charnoz. *The Astron. J.*, 154(1):34, 2017.
[13] M. Schaller, et al. *Proc. of PASC'16*, ACM, 2:1–10, 2016.
[14] J. H. Tillotson. Technical report, General Atomic, July 1963.
[15] D. J. Price. *J. Comp. Phys.*, 231:759–794, February 2012.
[16] M. Davis, et al. *Astrophys. J.*, 292:371–394, May 1985.